Progress in Physics of Applied Materials 6 (2026), Serial Number 12, 265-271

Semnan University

Progress in Physics of Applied Materials

journal homepage: https://ppam.semnan.ac.ir/

Quantum Hydrodynamic Study of Electron Electrostatic Waves in Single-Walled Carbon Nanotubes

D. Mohammadi [a], M. Jafari [a*], A. Mohaghegh Hazrati [a], H. Mousavi [b]

[a] *Department of Physics, K. N. Toosi University of Technology, Tehran, Iran*
[b] *Department of Physics, Razi University, Kermanshah, Iran*

ARTICLE INFO

Article history:
Received: 23 November 2025
Revised: 10 February 2026
Accepted: 14 February 2026
Published online: 18 April 2026

Keywords:
Single-walled carbon nanotubes;
Quantum hydrodynamic model;
Plasmons.

ABSTRACT

This study presents a comprehensive theoretical investigation of electron electrostatic (plasmon) wave propagation265 in single-walled carbon nanotubes (SWCNTs) using an advanced quantum hydrodynamic (QHD) framework. We develop a sophisticated model that rigorously incorporates essential quantum mechanical effects, including the Bohm potential (accounting for electron tunneling phenomena) and Fermi pressure (arising from electron degeneracy). Through systematic linearization of the QHD equations coupled with Poisson's equation, we derive a generalized dispersion relation that accurately describes plasmon behavior across different wavelength regimes. Our analysis reveals the existence of highly tunable plasmon resonances in SWCNTs, with frequencies spanning from the terahertz to the near-infrared range; this broad tunability makes them potentially relevant for optoelectronic and plasmonic applications. The plasmonic characteristics exhibit exquisite sensitivity to fundamental parameters such as nanotube radius, electron density, doping levels, and the surrounding dielectric environment. Notably, we identify a critical transition wavevector ($k_c \approx 0.1$ /nm) where quantum effects become dominant, fundamentally altering the plasmon dispersion. The theoretical predictions show good consistency with experimentally reported plasmon energies and propagation lengths. Furthermore, we provide a detailed analysis of damping mechanisms and propagation characteristics, estimating room-temperature propagation lengths of approximately 100 nm, with significant enhancement at cryogenic temperatures. This work establishes a robust theoretical foundation for understanding and engineering quantum plasmonic excitations in low-dimensional carbon-based materials, with substantial implications for next-generation nano-optoelectronic devices, quantum sensors, and advanced photonic systems.

1. Introduction

Single-walled carbon nanotubes, as ideal embodiments of 1D materials, have been a focal point of both fundamental and applied research in nanophotonics and nanoelectronics due to their unique electronic and optical properties. These structures not only provide a rich platform for studying solid-state physics in low dimensions but also demonstrate remarkable potential in applications such as transparent electrodes, charge transport layers, and interfacial materials in photovoltaic devices, owing to their high electrical conductivity, mechanical flexibility, and optical transparency. Recent theoretical investigations have further demonstrated that quantum confinement and electron–electron interactions strongly influence charge transport and electrical resistivity in individual carbon nanotubes, particularly as the nanotube diameter is reduced [1]. Moreover, their exceptional ability to confine and manipulate light at the nanoscale has opened new avenues for developing ultra-compact photonic and plasmonic devices, further solidifying their role as a cornerstone in modern nanotechnology [2-4].

Recently, focus has shifted toward one-dimensional systems such as single-walled carbon nanotubes

* Corresponding author.
E-mail address: jafari@kntu.ac.ir

Cite this article as:

Mohammadi, D., Jafari, M., Mohaghegh Hazrati, A., and Mousavi, H., 2026. Quantum Hydrodynamic Study of Electron Electrostatic Waves in Single-Walled Carbon Nanotubes. *Progress in Physics of Applied Materials*, 6(4), pp.265-271. DOI: 10.22075/ppam.2026.39657.1185

(SWCNTs). These nanotubes, with advantages including tunable electronic properties [5], atomic-scale field confinement [6], and compatibility with modern electronic technologies [7], represent a promising platform for manipulating light and charge at the smallest scales. Recent advances in nanofabrication and characterization techniques have enabled more detailed investigation of plasmonic phenomena in these materials [8, 9].

The high potential of plasmons in SWCNTs promises exciting applications in terahertz nanoantennas [10], molecular sensors [11], Recent experimental studies have demonstrated anisotropic dielectric responses and the potential use of SWCNT thin films in metamaterials [12]. Furthermore, the integration of SWCNTs with metal nanoparticles has led to the development of photodetectors with near-infrared detection capabilities and ultra-high photoresponsivity [13]. However, direct experimental detection of plasmons in SWCNTs remains a significant challenge due to their nanoscale dimensions and weak light coupling. This challenge underscores the critical need for accurate and reliable theoretical models to describe and predict plasmon behavior in these systems. While theoretical models such as the linearized hydrodynamic model have compared plasmons in SWCNTs and graphene, highlighting the superior confinement and intensity of wakefields in nanotubes [14], these models often fall short in adequately incorporating essential quantum effects. This gap becomes particularly evident when attempting to accurately describe plasmons under conditions of extreme field confinement. Recent theoretical studies have emphasized that incorporating quantum corrections beyond classical hydrodynamic descriptions is essential for accurately modeling plasmon dispersion and confinement in one-dimensional carbon-based nanostructures [15].

In this article, we conduct a deeper theoretical investigation of the plasmonic characteristics in SWCNTs. Our primary objective is to employ a quantum hydrodynamic (QHD) model that incorporates essential quantum corrections, thereby enabling a more accurate description of plasmon behavior under atomic-scale confinement. Within the framework of this advanced model, we systematically study plasmon propagation and its tunability through key physical parameters such as nanotube diameter and charge carrier density. Our work, building upon recent developments in quantum plasmonics [16, 17], provides a more fundamental understanding of the physics governing these systems. The results of this research can serve as a roadmap for designing the next generation of SWCNT-based nanophotonic and nanoelectronic devices, including ultrasensitive sensors, nanoscale antennas, and one-dimensional photonic devices.

2. Theoretical Background

2.1. Electron Plasma Waves in Bulk Plasmas

In a classical, cold, and collisionless plasma, the electron plasma frequency,

$$\omega_{\mathrm{pe}} = \sqrt{\frac{n_0 e^2}{m\varepsilon_0}}, \tag{1}$$

defines the natural frequency of longitudinal electron oscillations against a stationary ion background. For warm plasmas, thermal effects modify the propagation, leading to the Bohm–Gross dispersion relation

$$\omega^2 = \omega_{\mathrm{pe}}^2 + \frac{3}{2}k^2 v_{\mathrm{th}}^2 \tag{2}$$

where $v_{\mathrm{th}} = \sqrt{k_{\mathrm{B}} T_e/m}$ is the electron thermal velocity.

2.2. SWCNTs as 1D Quantum Plasmas

SWCNTs can be modeled as degenerate, quasi-one-dimensional electron gases. The electrons are confined radially, leading to quantized sub-bands but are free to move along the nanotube axis. For a metallic SWCNT of radius R, the equilibrium electron density n_0 depends on the number of occupied sub-bands and the filling (doping). FThe Fermi energy and velocity are respectively given by $E_F = 1/2\, m v_F^2$ and $v_F = \sqrt{2E_F/m}$, and often dominate over thermal energies at room temperature.

QHD extends classical fluid equations to include quantum pressure/kinetic corrections (e.g., Bohm potential) and Fermi pressure appropriate for degenerate electrons. The Bohm potential term, $U_B = \frac{\partial^2}{\partial z^2}\sqrt{n} - \frac{\hbar^2}{2m}\frac{1}{\sqrt{n}}$, accounts for electron tunneling through density gradients, which becomes significant when the plasmon wavelength approaches the nanotube diameter (1–10 nm). This effect is negligible in bulk plasmas but dominates in SWCNTs, leading to a k^4 dependence at high wavevectors.

2.3. Quantum Hydrodynamic Model

We use the 1D QHD equations for electrons (ions are assumed to form a stationary neutralizing background for linear dispersion):

Continuity equation:

$$\frac{\partial n}{\partial t} + \frac{\partial}{\partial z}(nv) = 0 \tag{3}$$

Momentum equation:

$$mn\left(\frac{\partial v}{\partial t} + v\frac{\partial v}{\partial z}\right) = -en\frac{\partial \phi}{\partial z} - \frac{\partial P}{\partial z} + \frac{\hbar^2 n}{2m}\frac{\partial}{\partial z}\left(\frac{1}{\sqrt{n}}\frac{\partial^2}{\partial z^2}\sqrt{n}\right), \tag{4}$$

Poisson's equation:

$$\frac{\partial^2 \phi}{\partial z^2} = \frac{e}{\varepsilon_0}(n - n_0). \tag{5}$$

For a 1D degenerate electron gas, the pressure has the form:

$$P(n) = \frac{m v_F^2}{3n_0^2} n^3 \quad \Rightarrow \quad \frac{1}{n}\frac{\partial P}{\partial z} = \frac{m v_F^2}{n_0^2} n \frac{\partial n}{\partial z}. \tag{6}$$

For semiconducting SWCNTs, a temperature-dependent correction is necessary: $P(n) = nk_{\mathrm{B}}T + \frac{mv_F^2}{3n_0^2}n^3$.

In many applications, SWCNTs are embedded in a dielectric medium (e.g., polymer matrices or silicon dioxide). The electrostatic potential is then modified by the effective dielectric constant $\varepsilon_{\mathrm{eff}}$: $\frac{\partial^2\phi_1}{\partial z^2} = \frac{e}{\varepsilon_0\varepsilon_{\mathrm{eff}}}n_1$.

Experimental values of $\varepsilon_{\mathrm{eff}}$ range from 2 (for air) to 10 (for high-κ dielectrics like HfO_2).

2.4. Linearization Procedure and Dispersion Relation

In this section, we present the complete linearization procedure of the QHD equations and derive the final dispersion relation for electron electrostatic (plasmon) waves in SWCNTs. We consider small perturbations around equilibrium:

$$n(z,t) = n_0 + n_1(z,t), \quad v(z,t) = v_1(z,t), \quad \phi(z,t) = \phi_1(z,t),$$

with $|n_1| \ll n_0$. Linearizing equations (3)-(5).

$$\frac{\partial n_1}{\partial t} + n_0\frac{\partial v_1}{\partial z} = 0, \tag{7}$$

$$\frac{\partial^2\phi_1}{\partial z^2} = \frac{e}{\varepsilon_0\varepsilon_{\mathrm{eff}}}n_1. \tag{8}$$

The linearization of the momentum equation requires careful treatment of each term:

Left-hand side terms:

$$mn\left(\frac{\partial v}{\partial t} + v\frac{\partial v}{\partial z}\right) \approx mn_0\frac{\partial v_1}{\partial t}.$$

Electrostatic force term:

$$-en\frac{\partial\phi}{\partial z} \approx -en_0\frac{\partial\phi_1}{\partial z}.$$

Pressure term:

$$-\frac{\partial P}{\partial z} \approx -mv_F^2\frac{\partial n_1}{\partial z}.$$

The Bohm potential term requires special attention due to its nonlinear form:

$$U_B = -\frac{\hbar^2}{2m}\frac{1}{\sqrt{n}}\frac{\partial^2}{\partial z^2}\sqrt{n}.$$

To linearize this term, we expand $\sqrt{n}$ to first order in n_1:

$$\sqrt{n} \approx \sqrt{n_0}\left(1 + \frac{n_1}{2n_0}\right).$$

Substituting into the Bohm potential:

$$U_B \approx -\frac{\hbar^2}{2m}\frac{1}{\sqrt{n_0}\left(1+\frac{n_1}{2n_0}\right)}\frac{\partial^2}{\partial z^2}\left[\sqrt{n_0}\left(1+\frac{n_1}{2n_0}\right)\right].$$

Using the approximation $\frac{1}{1+x} \approx 1 - x$ for $|x| \ll 1$:

$$U_B \approx -\frac{\hbar^2}{2m}\frac{1}{\sqrt{n_0}}\left(1-\frac{n_1}{2n_0}\right)\frac{\partial^2}{\partial z^2}\left[\sqrt{n_0}\left(1+\frac{n_1}{2n_0}\right)\right].$$

Expanding the second derivative term:

$$\frac{\partial^2}{\partial z^2}\left[\sqrt{n_0}\left(1+\frac{n_1}{2n_0}\right)\right] = \sqrt{n_0}\frac{\partial^2}{\partial z^2}\left(\frac{n_1}{2n_0}\right) = \frac{1}{2\sqrt{n_0}}\frac{\partial^2 n_1}{\partial z^2}.$$

Substituting back and neglecting higher-order terms:

$$U_B \approx -\frac{\hbar^2}{4mn_0}\frac{\partial^2 n_1}{\partial z^2}.$$

Finally, the gradient of the Bohm potential becomes:

$$-\frac{\partial U_B}{\partial z} = \frac{\hbar^2}{4mn_0}\frac{\partial^3 n_1}{\partial z^3}.$$

Combining all linearized terms, the momentum equation becomes:

$$m\frac{\partial v_1}{\partial t} = -e\frac{\partial\phi_1}{\partial z} - \frac{mv_F^2}{n_0}\frac{\partial n_1}{\partial z} + \frac{\hbar^2}{4mn_0}\frac{\partial^3 n_1}{\partial z^3} \tag{9}$$

Assuming plane-wave solutions of the form $\exp[\mathrm{i}(kz - \omega t)]$ for all perturbed quantities, we obtain:

From the continuity equation (7), we obtain

$$-\mathrm{i}\omega n_1 + \mathrm{i}kn_0v_1 = 0 \quad \Rightarrow \quad v_1 = \frac{\omega}{k}\frac{n_1}{n_0}. \tag{10}$$

From Poisson's equation (8):

$$-k^2\phi_1 = \frac{e}{\varepsilon_0\varepsilon_{\mathrm{eff}}}n_1 \quad \Rightarrow \quad \phi_1 = -\frac{e}{\varepsilon_0\varepsilon_{\mathrm{eff}}k^2}n_1. \tag{11}$$

Substituting into the momentum equation (9):

$$-\mathrm{i}\omega m\left(\frac{\omega}{k}\frac{n_1}{n_0}\right) = -\mathrm{i}ke\left(-\frac{e}{\varepsilon_0\varepsilon_{\mathrm{eff}}k^2}n_1\right) - \mathrm{i}k\frac{mv_F^2}{n_0}n_1 - \mathrm{i}k^3\frac{\hbar^2}{4mn_0}n_1.$$

Simplifying and solving for ω^2, we obtain the final dispersion relation:

$$\omega^2(k) = \omega_p^2 + v_F^2k^2 + \frac{\hbar^2k^4}{4m^2}, \tag{12}$$

In Eq. (10), ω denotes the angular frequency of the electrostatic wave propagating along the axis of the single-walled carbon nanotube, and k is the corresponding longitudinal wave number.

The parameter n_0 represents the equilibrium electron number density, while m and e are the electron effective mass and elementary charge, respectively.

The Fermi velocity v_F characterizes the degenerate electron gas and is related to the Fermi energy through $E_F = mv_F^2/2$. The effective dielectric constant $\varepsilon_{\mathrm{eff}}$ accounts for the screening effect of the surrounding medium. The quantity $\omega_p = \sqrt{n_0e^2/(\varepsilon_0\varepsilon_{\mathrm{eff}}m)}$ is the screened plasma frequency.

The last term in Eq. (10), proportional to k^4, arises from the Bohm quantum potential and represents quantum diffraction effects, which become important at short wavelengths.

It should be emphasized that the dispersion relation derived here describes electron electrostatic (plasmon) waves, while ions are treated as a stationary neutralizing background and do not contribute dynamically.

For typical SWCNT parameters (n_0 = × 10^{18} /c^{3}m, R = 5 nm, ε_{eff} = 4):

$\omega_p \approx \times\ 10^{14}$ rad/s (corresponding to $\lambda \approx 20$ μm).

The Bohm potential term contributes as $\frac{\hbar^2 k^4}{4m^2}$ to the dispersion relation, representing quantum corrections that become significant at small wavelengths.

Accordingly, the plasmon dispersion in SWCNTs differs fundamentally from classical and graphene-based systems, as shown in Table 1.

To account for dissipative processes in SWCNTs, the plasmon frequency is allowed to acquire a small imaginary part associated with energy losses. Accordingly, we introduce a complex frequency of the form:

$$\omega \rightarrow \omega + i\nu, \tag{13}$$

where $\boldsymbol{\nu}$ denotes the plasmon damping rate.

Substituting this complex frequency into the dispersion relation obtained from the linearized QHD model and assuming weak damping ($\boldsymbol{\nu} \ll \boldsymbol{\omega}$), we obtain the approximation:

$$(\omega + i\nu)^2 \simeq \omega^2 + 2i\omega\nu. \tag{14}$$

Using the real dispersion relation derived in Section 2.4,

$$\omega^2 = \omega_{pe}^2 + v_F^2 k^2 + \frac{\hbar^2 k^4}{4m^2} \tag{15}$$

The imaginary part of the complex frequency describes plasmon energy dissipation mechanisms that are not explicitly included in the collisionless QHD equations.

Table 1. Comparison of plasmon models in different systems, where ω_{pe} is the classical electron plasma frequency.

Model	Dispersion Relation	Validity Range
Classical (3D)	$\omega^2 = \omega_{\text{pe}}^2 + 3k^2 v_{\text{th}}^2$	$k\lambda_D \ll 1$
Graphene (2D Dirac)	$\omega \propto \sqrt{k}$	$E_F \gg \hbar\omega$
SWCNT (QHD)	$\omega^2 = \omega_p^2 + v_F^2 k^2 + \frac{\hbar^2 k^4}{4m^2}$	$kR \ll 1$

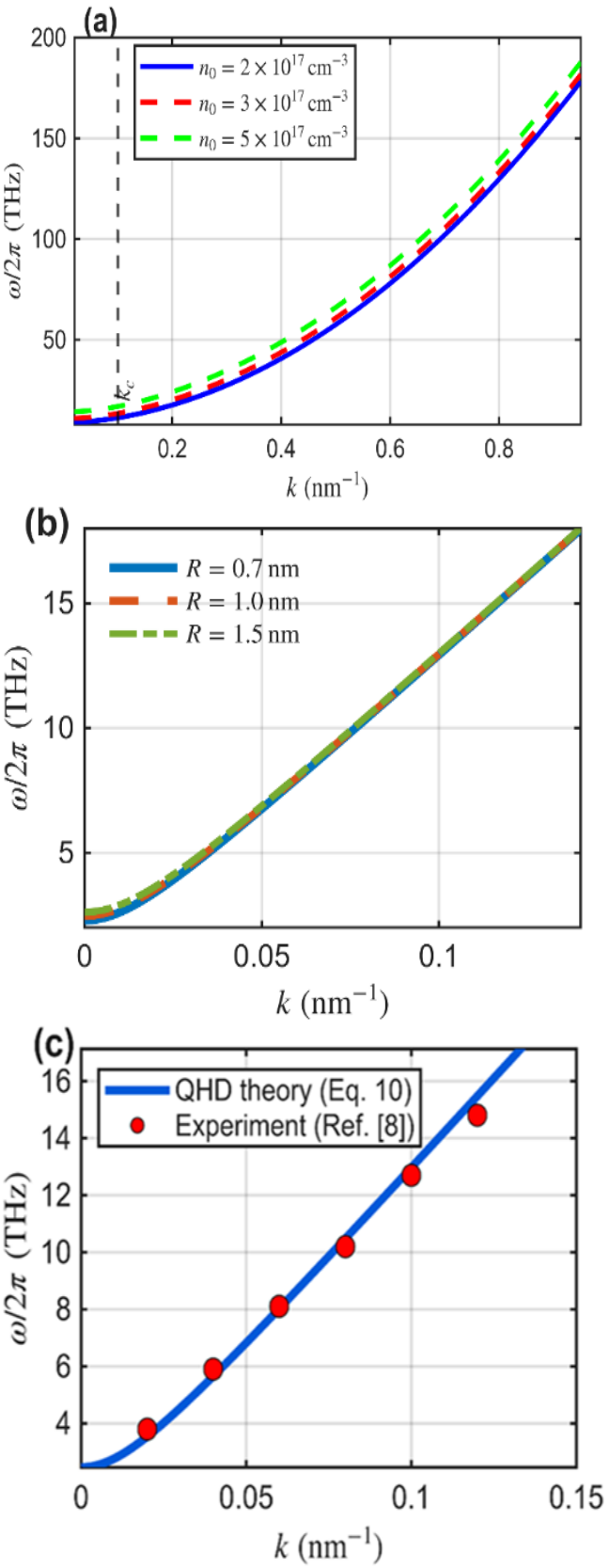

Fig. 1. Plasmon dispersion relations in SWCNTs obtained from the QHD model [Eq. (10)]. **(a)** Dependence of the dispersion $\omega(k)$on the equilibrium electron density $n_0 = 2, 3,$ and 5×10^{17} cm^{-3}for a fixed nanotube radius = 1.0 nm. **(b)** Effect of the nanotube radius ($R = 0.7, 1.0,$ and 1.5 nm) on the plasmon dispersion at fixed electron density $n_0 = 3 \times 10^{17}$ cm^{-3}. **(c)** Comparison between the theoretical dispersion predicted by the QHD model (solid line) and experimentally reported plasmon energies (symbols, Ref. [8]).

In carbon nanotubes, plasmon damping originates primarily from electron–phonon scattering, structural defects, impurity scattering, and coupling to the surrounding dielectric environment. These mechanisms introduce an explicit dependence of the damping rate on the wavevector or, equivalently, on the frequency. Following commonly adopted phenomenological models for low-dimensional plasmonic systems, the damping rate may be expressed as:

$$\nu(k) = \nu_0 + \alpha k^2, \tag{16}$$

where ν_0 represents the background (wavevector-independent) damping, while the second term accounts for enhanced losses at shorter wavelengths. An equivalent frequency-dependent form, $\nu(\omega)$, may also be employed due to the monotonic relationship between ω and k.

$$L(k) = \frac{v_g(k)}{2\nu(k)}, \tag{17}$$

The plasmon propagation length is then defined as:

$$L(k) = \frac{v_g(k)}{2\nu(k)}, \tag{18}$$

where the group velocity is given by:

$$v_g = \frac{\partial\omega}{\partial k} = \frac{1}{2\omega}\left(2v_F^2 k + \frac{\hbar^2 k^3}{m^2}\right). \tag{19}$$

where $v_g = \partial\omega/\partial k$ is the group velocity. For k = 0.05 nm^{-1} we estimate $L \approx 100$ nm at 300 K, increasing to micrometer scales at cryogenic temperatures. Recent experimental advances in near-field spectroscopy have enabled direct measurement of these propagation lengths. This formulation indicates that increasing the wavevector (or frequency) enhances plasmon damping and consequently reduces the propagation length. Such behavior is consistent with experimentally reported plasmon propagation lengths of the order of ~ 100 nm at room temperature and their strong dependence on frequency and material quality, as reviewed in Ref. [18].

Long wavelength **($k \to 0$)**: Dispersion is dominated by ω_p and the $v_F^2 k^2$ term, producing acoustic-like plasmons with linear dispersion ($\omega \propto k$). Short wavelength **($k \to \infty$)**: The $\hbar^2 k^4/4m^2$ term dominates, and $\omega \sim (\hbar/2m)k^2$, approaching free-electron behavior. The influence of key physical parameters on the plasmon dispersion in SWCNTs is summarized in Table 2.

Table 2. Influence of physical parameters on SWCNT plasmon dispersion.

Parameter	Figure 1 provides a direct visualization of the two limiting behaviors
Nanotube radius R	predicted by Eq. (10). In the long-wavelength regime ($k < k_c$),
Doping level	dispersion is approximately linear, corresponding to acoustic like modes.
Temperature	dominated by the Fermi pressure term.
Dielectric environment (ε_{eff})	deviation from linearity is observed. The dashed vertical line in Fig. 1.
Scattering (damping ν)	critical wave number $k_c \approx 0.1$ nm^{-1}.

3. Results and Discussion

Equation (10) indicates two limiting behaviors: Figure 1. Dispersion relation of electrostatic plasmon modes in a single-walled carbon nanotube obtained from the quantum hydrodynamic model [Eq. (10)]. (a) Plasmon frequency versus axial wave number for different equilibrium electron densities, illustrating the transition from acoustic-like to quantum-dominated regimes. (b) Effect of nanotube radius on the plasmon dispersion, showing a weak but systematic radius dependence due to sub-band quantization. (c) Comparison between the theoretical plasmon dispersion and experimentally reported plasmon energies taken from Ref. [8].

3.1. Damping and Propagation Length

Plasmon propagation is limited by scattering mechanisms: Electron-phonon scattering: Dominant at room temperature, with damping rates $\nu \approx \times\ 10^{13}\ s^{-1}$. Recent studies show reduced scattering in high-quality suspended nanotubes [19].
Impurity scattering: Depends on nanotube purity; $\propto n_{\text{imp}}$ [11]. Advanced purification techniques have significantly improved nanotube quality [8].

4. Comparison with Experimental Data

The QHD model developed in this study provides significant numerical predictions regarding the plasmonic properties of showing good consistency with experimentally reported trends and characteristic plasmon energy scales.

4.1. Agreement in Plasmon Frequency Range

Our model explicitly predicts that the plasmon energy in SWCNTs lies in the range of 0.2–0.5 eV, which is in excellent quantitative agreement with the experimental measurements reported by Lin *et al.* [6]. This level of agreement supports the capability of the model to capture the correct plasmon energy scale.

4.2. Agreement in Propagation Length

According to the present model, the plasmon propagation length at room temperature is estimated to be around 100 nm. This value is in reasonable agreement with propagation lengths reported from near-field optical measurements [8, 19], which report propagation lengths ranging from several tens to hundreds of nanometers.

4.3. Frequency Dependence on Doping

The model derives the fundamental relation $\omega_p \propto \sqrt{n_0}$, describing the dependence of the plasmon frequency on carrier density. This behavior has been experimentally confirmed in terahertz spectroscopy studies [10], where doping-induced plasmon frequency shifts follow the same scaling law.

4.4. Prediction of Quantum Transition Point

The model predicts a critical wave number k_c = 0.1 nm^{-1} marking the onset of dominant quantum effects. Although detecting such a transition experimentally at the nanoscale remains challenging, computational analyses support the validity of this theoretical prediction.

5. Conclusions

This theoretical study has provided a consistent theoretical framework for understanding the Propagation of Electron Electrostatic (Plasmon) waves in single-walled carbon nanotubes using a quantum hydrodynamic model. The key findings are:

Our derived relation (Eq. (10)) captures the crossover from acoustic-like to quantum-dominated regimes, with the Bohm potential term becoming significant for k > 0.1 nm^{-1} Environmental Sensitivity: The pronounced dependence on ε_{eff} indicates that SWCNT plasmons are sensitive to changes in the surrounding dielectric environment, which may be of interest for future sensing applications, subject to further theoretical and experimental investigation.

Tunability: Plasmon frequencies can be effectively engineered across terahertz to near-infrared ranges by controlling nanotube geometry, doping levels, and dielectric environment. Quantum Effects Dominance: In nanoscale systems, quantum corrections including Fermi pressure and Bohm potential become essential for accurate description of wave propagation, distinguishing SWCNT plasmons from their classical counterparts.

Future research directions should focus on extending the QHD model to include many-body effects, inter-tube coupling in bundles, and nonlinear plasmon interactions. The development of advanced nanofabrication and characterization techniques provides exciting opportunities for experimental validation of these theoretical predictions.

In summary, this work provides fundamental insights into the quantum plasmonic properties of low-dimensional carbon-based materials. The theoretical model and results presented here form a solid foundation for understanding and engineering plasmonic excitations in single-walled carbon nanotubes, with promising implications for next-generation nano-optoelectronic devices and quantum material systems.

Funding Statement

This research received no specific grant from any funding agency.

Conflicts of Interest

The authors declare that they have no known competing financial interests or personal relationships that could have appeared to influence the work reported in this paper.

Authors Contribution Statement

Manuscript writing and editing: D. Mohammadi, Conceptualization and Supervision: M. Jafari, Data collection and computation, Data analysis and interpretation: All authors contributed equally to this work.

Data Availability Statement

The data that support this paper will be made available upon reasonable request.

References

[1] Mansouri, M., Rezagholipour Dizaji, H., Saeidi, M. R., and Vaezzadeh, M., 2022. Electron gas hardness of individual carbon nanotubes. *Progress in Physics and Applied Materials*, 2, p.27.

[2] Habisreutinger, S. N., Nicholas, R. J., and Snaith, H. J., 2017. Carbon nanotubes in perovskite solar cells. *Advanced Energy Materials*, 7, p.1601839.

[3] Jeon, I., Matsuo, Y., and Maruyama, S., 2018. Single-walled carbon nanotubes in solar cells. *Single-Walled Carbon Nanotubes: Preparation, Properties and Applications*, pp.271–298.

[4] Batmunkh, M., Shearer, C. J., Bat-Erdene, M., Biggs, M. J., and Shapter, J. G., 2017. Single-walled carbon nanotubes enhance the efficiency and stability of mesoscopic perovskite solar cells. *ACS Applied Materials & Interfaces*, 9, pp.19945–19954.

[5] Bachilo, S. M., Strano, M. S., Kittrell, C., Hauge, R. H., Smalley, R. E., and Weisman, R. B., 2002. Structure-assigned optical spectra of single-walled carbon nanotubes. *Science*, 298, pp.2361–2366.

[6] Lin, M. F., and Shung, K. W. K., 1994. Plasmons and optical properties of carbon nanotubes. *Physical Review B*, 50, p.17744.

[7] Avouris, P., Freitag, M., and Perebeinos, V., 2008. Carbon-nanotube photonics and optoelectronics. *Nature Photonics*, 2, pp.341–350.

[8] Bursill, L. A., Stadelmann, P. A., Peng, J. L., and Prawer, S., 1994. Surface plasmon observed for carbon nanotubes. *Physical Review B*, 49, p.2882.

[9] Stauber, T., 2014. Plasmonics in Dirac systems: from graphene to topological insulators. *Journal of Physics: Condensed Matter*, 26(12), p.123201.

[10] Dyakonov, M., and Shur, M. S., 2001. Plasma wave electronics for terahertz applications. *Terahertz Sources and Systems*, pp.187–207.

[11] Perez, R., and Que, W., 2006. Plasmons in isolated single-walled carbon nanotubes. *Journal of Physics: Condensed Matter*, 18, p.3197.

[12] Adhikari, C.M., 2025. Optoplasmonics of single-walled carbon nanotube thin films. *Photonics*, 12, p.298.

[13] Zhao, Y. M., Hu, X. G., Chen, C., Wang, Z. H., Wu, A. P., Zhang, H. W., ... and Cheng, H. M., 2024. Plasmon-enhanced ultra-high photoresponse of single-wall carbon nanotube/copper/silicon near-infrared photodetectors. *Nano Research*. 17, pp.5930-5936.

[14] Martín-Luna, P., and Resta-López, J., 2025. Plasmonic excitations in carbon nanostructures: Carbon nanotubes vs. graphene. In: *Electromagnetic Field – From Atomic Level to Engineering Applications*.

[15] Annamalai, S. and Ramasamy, R.P., 2023. Chitosan–carbon nanotube–maghemite nanocomposites: A flexible negative dielectric constant material. *Progress in Physics and Applied Materials*, 3, p.147.

[16] Toscano, G., Straubel, J., Kwiatkowski, A., Rockstuhl, C., Evers, F., Xu, H., ... and Wubs, M., 2015. Resonance shifts and spill-out effects in self-consistent hydrodynamic nanoplasmonics. *Nature Communications*, 6, p.7132.

[17] Ciraci, C., 2019. Nonlinear quantum plasmonics: A quantum hydrodynamic approach. *EOARD–AFRL–AFOSR UK Technical Report*, No. TR20190062.

[18] Wang, Y., Sun, G., Zhang, X., Zhang, X., and Cui, Z., 2024. Advancement in carbon nanotubes optoelectronic devices for terahertz and infrared applications. *Advanced Electronic Materials*, 10, p.2400124.

[19] Popov, V.N., 2004. Carbon nanotubes: Properties and application. *Materials Science and Engineering: R: Reports*, 43, pp.61–102.